SASBE 2025 aims to encourage the international exchange of innovative ideas between researchers from academia and industry. In addition to knowledge dissemination, the conference offers a valuable platform for professional networking, particularly benefiting university professors, graduate students, and postdoctoral researchers.

Research Article

Validation of Computational Fluid Dynamic in Simulating Urban Water's Cooling Effect in Subtropical Climate Area

Shun-Yu Yang[1], Ying-Chieh Chan[2]

1 Master Student, Department of Civil Engineering, National Taiwan University, Taipei, Taiwan.
2 Associate Professor, Department of Civil Engineering, National Taiwan University, Taipei, Taiwan.
Correspondence: r12521716@g.ntu.edu.tw

Abstract

Urban water bodies mitigate near-surface heat through evaporation and thermal storage, yet their performance is under-validated in hot–humid settings. This study evaluates Computational Fluid Dynamic software (CFD) for simulating lake-induced cooling on the National Taiwan University campus (Taipei) and quantifies the trade-off between grid resolution, accuracy, and computational cost. We first performed a grid-size verification using 3, 6, and 9 m cells for scenario with and without Drunken Moon Lake, analysing grid size effect on air temperature (AT), relative humidity (RH), specific humidity (SH), wind speed (WS), wind direction (WD), and mean radiant temperature (MRT). We then applied the optimal resolution to validate simulations against four field measurements at two sites, using time-series and scatter analyses. Grid verification showed consistent lake cooling in AT and MRT across all resolutions; RH and SH differences were small, and WS/WD were comparatively insensitive to grid size. A 24-hr simulation required 84.5 hr (3 m), 13 hr (6 m), and 6.5 hr (9 m), indicating 6 m as a pragmatic resolution that preserves the lake signal while reducing runtime by more than 6 times relative to 3 m. Validation result demonstrated high agreement for AT, moderate-to-strong performance for RH and SH, and weak, positively biased WS with low correlation. The study fills a blue-infrastructure validation gap and offers actionable guidance on grid selection for campus and district-scale applications. In practice, CFD software use in this research under grid size setting at 6 m supports climate-sensitive design focused on thermal outcomes; wind-dependent decisions should be complemented by other higher-order computational fluid dynamics or targeted monitoring. Limitations include short monitoring windows, two validation sites, and generalized vegetation–water parameters. Findings from this research can inform resilient design and policy for water-based cooling in hot–humid cities.

Keywords: Blue infrastructure; Climate Change Adaptation, Microclimate Simulation, Computational Fluid Dynamics (CFD)

Highlights

- CFD software (ENVI-met) captures lake-induced cooling in AT/MRT; RH/SH effects are modest; wind-speed skill is weak.
- Blue-infrastructure cooling validated in a hot–humid campus setting.
- A 6 m grid preserves the lake signal and reduces runtime by more than 6 times compared with 3 m.

1 Introduction

Urban Heat Island (UHI) effects have intensified with climate change and rapid urbanisation(Richa Jain, 2022). Dense urban fabrics which characterised by high thermal mass, low albedo, and limited evapotranspiration, makes cites absorb and store solar energy, leading to higher air and surface temperatures compare to surrounding rural areas(Liu et al., 2024; Tian et al., 2021). These temperature elevations are linked to increased energy and water demand in buildings, degraded air quality, and reduced outdoor thermal comfort(Tian et al., 2021).

A wide range of strategies has been proposed to mitigate UHI, including vegetation-based measures (e.g., trees, green roofs and façades), water-based interventions (e.g., ponds, lakes, channels), urban form and planning approaches (e.g., ventilation corridors, shading from morphology), and material solutions (e.g., high-albedo or high-emissivity pavements) (Ren et al., 2023). While the thermal benefits of greening are well documented, the magnitude and spatial extent of cooling provided by blue infrastructure remain less consistently quantified across climates and urban morphologies(Liu et al., 2021). The specific evidence of water body's effect is therefore needed, to support design decisions and policy. This paper investigates whether ENVI-met can reliably in simulate lake-induced cooling effect in a hot and humidity campus and what grid resolution balances accuracy and runtime for design use. Results include (i) verify resolution sensitivities and (ii) validate simulations result of Air Temperature (AT), Relative Humidity (RH), Specific Humidity (SH) and Wind Speed (WS) against four different data from site measurement, reporting performance via R^2, RMSE, and MAPE.

2 A Review on Computational Fluid Dynamics in Water Cooling Effect

This section establishes the theoretical and empirical foundation for our study by clarifying core concepts and positioning ENVI-met software within the broader Computational Fluid Dynamics (CFD) based urban microclimate literature. First, we analysis the difference between the CFD software. Then summarize synthesise existing frameworks and evidence on ENVI-met's performance.

2.1 Computational Fluid Dynamics

Computational Fluid Dynamics is widely used to assess urban microclimates since it isolates the influence of individual parameters, enables controlled scenario testing, and provides spatially continuous fields rather than point measurements (Ampatzidis & Kershaw, 2020; Toparlar et al., 2017). In microclimate study there are several popular CFD software, Table 1 compare several widely used CFD platforms, highlight their applications, strengths, limitations, and sets in water simulation (Le et al., 2024). Alternative CFD approaches, such as ANSYS Flurent or OpenFOAM, offer higher flexibility in turbulence modelling but often require greater computational resources and specialized expertise. ENVI-met's balance of usability and specificity has made it the dominant model for microclimate research. From previous review of CFD models being used, almost half of the investigated studies were based on ENVI-met (Adilkhanova et al., 2022; Pignatta et al., 2018; Toparlar et al., 2017). ENVI-met is a three-dimensional, grid-based, non-hydrostatic model that simulates coupled exchanges of momentum, heat, and moisture between buildings, vegetation, and the atmosphere, drawing on the fundamental laws of fluid dynamics and thermodynamics (Sinsel, 2022). This makes it a powerful tool for assessing changes in urban thermal environment, though questions remain about its accuracy in underexplored scenarios such as water body cooling effect.

Table I. Comparison of common Computational Fluid Dynamic software

Software	Applications	Advantages	Limitations	Water Simulation
ENVI-met	Urban microclimate, UHI analysis, evaluation of green infrastructure	Designed specifically for urban microclimate studies; includes eight built-in databases offers a convenient starting point; suitable for assessing UHI mitigation strategies such as green roofs and vertical greening	Default settings are optimized for temperate climates; simulations in subtropical/tropical contexts require localization adjustments; potential overestimation of temperature and simplified radiation flux calculations	Treats water as fixed surface; models radiation and evaporation; simplified shallow-water energy balance; no free-surface hydrodynamics capabilities.
ANSYS-Fluent	Microclimate and energy balance (e.g., radiation, evapotranspiration, surface temperature)	High flexibility; offers multiple turbulence models, radiation schemes, and mesh configurations; capable of high-accuracy simulations for complex energy balance studies	No dedicated urban database; vegetation and soil parameters must be manually defined; porous media approaches for foliage may inadequately represent shading; computationally intensive with complex setup	Use Volume of Fluid (VOF) for air–water interfaces; couples' species-based evaporation with heat transfer.
OpenFOAM	Urban wind field and wind energy analyses	Open-source software; fully customizable code; highly flexible for diverse CFD problems	No built-in material or vegetation database; requires user-defined coding; steep learning curve and high development cost	Uses interFoam VOF to track interfaces; optional phase-change libraries; configurable radiation coupling.
PHOENICS	Urban wind environment analysis	Fast computation; efficient for city-scale wind field simulations; provides partial building and thermal parameters	Limited databases; weak support for ground and vegetation processes; requires user-provided measurements or parameters	Offers VOF and Scalar-Equation free-surface schemes; optional Continuum Surface Force

2.2 Past Water Body's Simulation Result

Prior simulations of water bodies report consistent, context-dependent cooling. Using CFD, Tominaga et al. (2015) validated evaporative cooling from urban water surfaces and found pedestrian-level air temperature reductions of about 2 °C, with the cooling plume extending to 100 m downwind in the absence of obstructions. Shi et al.(2020) quantified blue–green synergies, showing that a one-unit decrease in tree LAI around water was associated with 0.19–0.31 °C lower average air temperature, and reporting greater cooling for species with lower LAI in waterfront settings. At campus scale, Ampatzidis and Kershaw (2020) simulated around 1 °C cooling attributable to water bodies, whereas Liao et al. (2024) observed stronger seasonal asymmetry in a subtropical campus, up to 3.5 °C daytime cooling in summer and 3.9 °C daytime warming in winter near water due to radiative–advective effects. Comparative analyses also indicate air-temperature reductions of 1.6 °C from vegetation and 1.1 °C from ponds (Adilkhanova et al., 2022).

2.3 Knowledge Gaps and Research Opportunities

Despite extensive use, the past ENVI-met literature is strongly skewed toward greening appear in 70% of studies, whereas water bodies are addressed in only 5% (Liu et al., 2021). Moreover, validation remains inconsistent, a recent review found that most CFD urban microclimate studies lacked observational validation (105 of 183), raising concerns about reliability and transferability (Tominaga et al., 2015; Toparlar et al., 2017). These gaps motivate targeted validation of ENVI-met for blue infrastructure in subtropical area's settings and a clearer understanding of resolution accuracy trade-offs for future decision support.

3 Methodology

In this research, we adopt a four-step framework: (i) field data collection, (ii) model build and grid-size verification simulaiton (with grid size: 3m, 6m, 9 m), (iii) validation against four on-site collected data, using time-series comparison and R^2, RMSE and MAPE, (iv) result analysis in outcomes. This structure directly addresses the literature's two central needs: validated evidence for water-body cooling and practical guidance on model resolution for district-scale water applications.

3.1 Field Measurements

Field data collect were conducted around Drunken Moon Lake at National Taiwan University, central Taipei (Figure 1.). Two sites were monitored (Figure 1. iii), Site A (near lakeside) and Site B (open grassland). Sensors (Table 2.) were installed at pedestrian height (1.5 m) to capture AT, RH, and WS. SH was derived from air temperature, relative humidity, and air pressure (≈1013 hPa). Four days' site measurement were conducted from V1 to V4. Table 3. Shows the detail of each site collect.

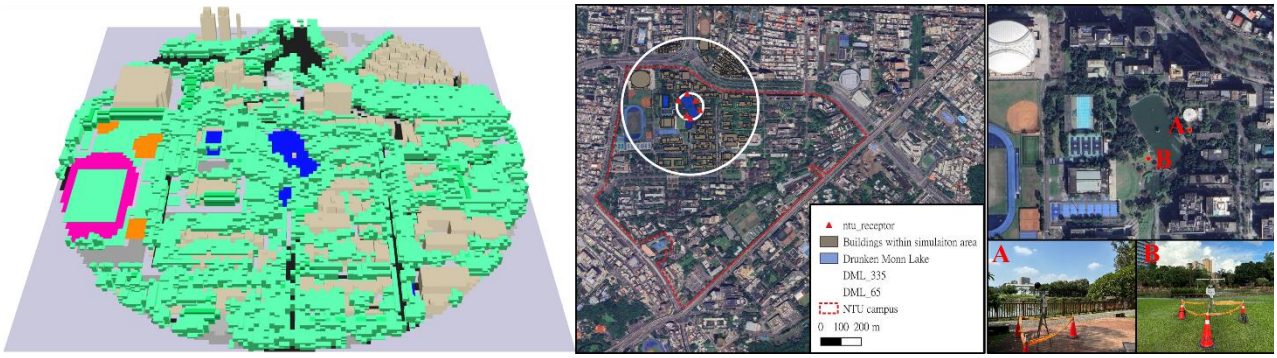

(i) (ii) (iii)

Figure 1. Study area and measurement setup: (i) ENVI-met simulation model, (ii) site location at National Taiwan University with simulation domain and Drunken Moon Lake, and (iii) measurement points A and B around Drunken Moon Lake with corresponding field instrumentation.

Table 2. Measurement variables, technical information of instrument

Variable	Sensor	Accuracy	Measurement Range	Output resolution	Sampling
Air temperature (AT)	HOBO S-THC-M002	±0.25°C (from -40° to 0°C) ±0.20°C (from 0° to 70°C)	-40°C to 75°C	0.02°C	5 min
Relative humidity (RH)	HOBO S-THC-M002	±2.5% (from 10% to 90% RH)	0-100%* RH at -40° to 75°C	0.01% RH	5 min
Wind speed (WS)	HOBO S-WSB-M003	± 1.1 m/s or ± 4% of reading whichever is greater	0 to 76 m/s	0.5 m/s	5 min
Solar radiation	HOBO S-LIB-M003	±10 W/m2 or ±5%,	0 to 1280 W/m2	1.25 W/m2	5 min
Data logger	HOBO H21-USB		-20° to 50°C	1 second to 18 hours	

Table 3. Summary of field measurement, including case period, measurement site, and weather conditions.

Case	Time	Site	Weather condition
V1	2024/10/18 00:00 – 2024/10/19 15:00 (39hr)	A	Sunny
V2	2024/10/19 16:00 – 2024/10/21 07:00 (39hr)	B	Sunny, cloudy afternoon
V3	2025/03/25 00:00 – 2025/03/25 22:00 (22hr)	B	Sunny
V4	2025/03/26 00:00 – 2025/03/26 22:00 (22hr)	A	Sunny

3.2 Simulation Model Build and Weather Input

CFD simulation model with domain centred on Drunken Moon Lake; 5 times Drunken Moon Lake's radius with 10-grid buffer to limit boundary artefacts were build (Figure 1. i). Vegetation was explicitly

represented. 2631 trees were included in domain, of which 1754 were matched to the ENVI-met database by morphological similarity (e.g., crown diameter, height, leaf density). The remaining 877 trees were generalized using “Tree of Heaven” as a representative species. To ensure stable boundary conditions, each simulation included a 6-hour spin-up period prior to the validation period. Simulation weather input file are shown as Figure 3.

As Figure 2. Shown, six scenarios combine 3/6/9 m grids with and without lake, outputs from six points for AT, RH, SH, WS, WD and MRT, data were compared to quantify parameter sensitivity in gird size change, lake signal robustness, and computational cost.

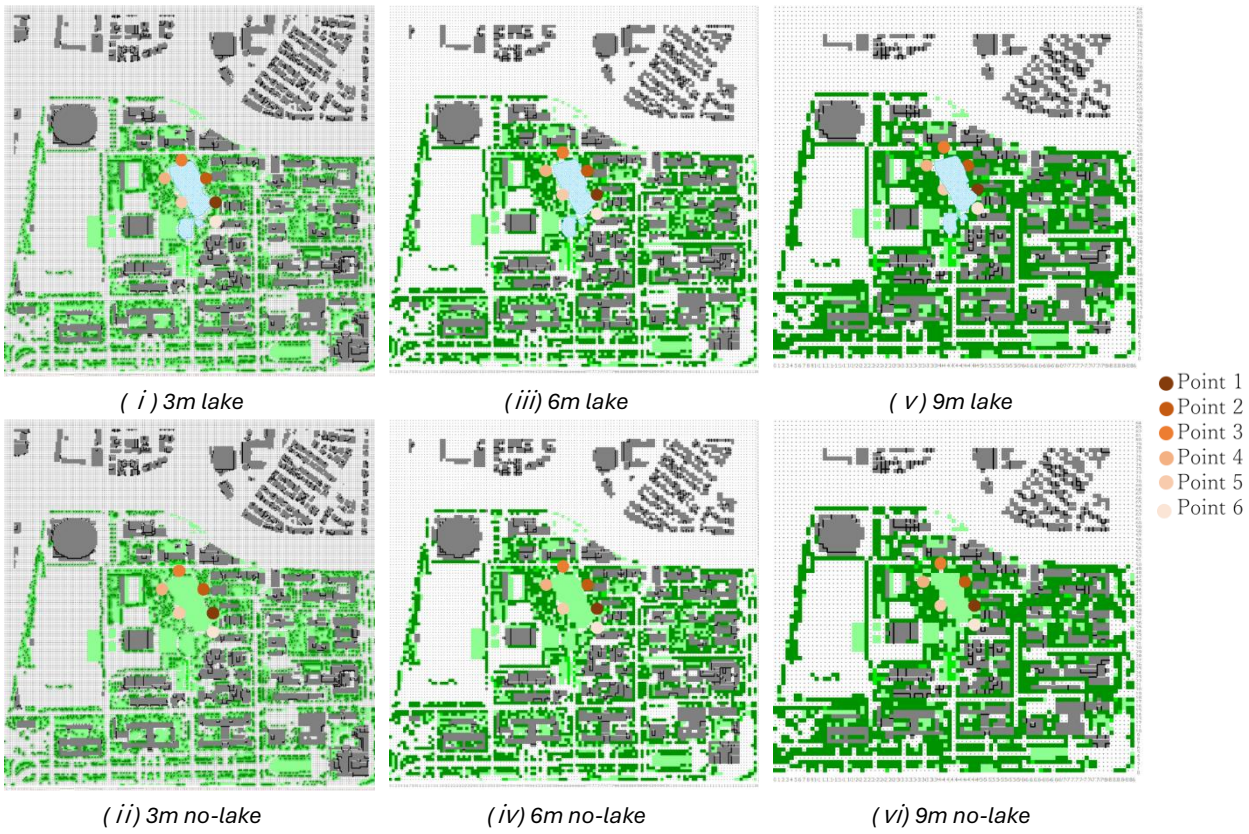

(i) 3m lake (iii) 6m lake (v) 9m lake

(ii) 3m no-lake (iv) 6m no-lake (vi) 9m no-lake

Figure 2. Spatial distribution of simulated microclimate at Point 1–6 under different grid sizes and water-body settings: (i) 3 m lake, (ii) 3 m no-lake, (iii) 6 m lake, (iv) 6 m no-lake, (v) 9 m lake, and (vi) 9 m no-lake.

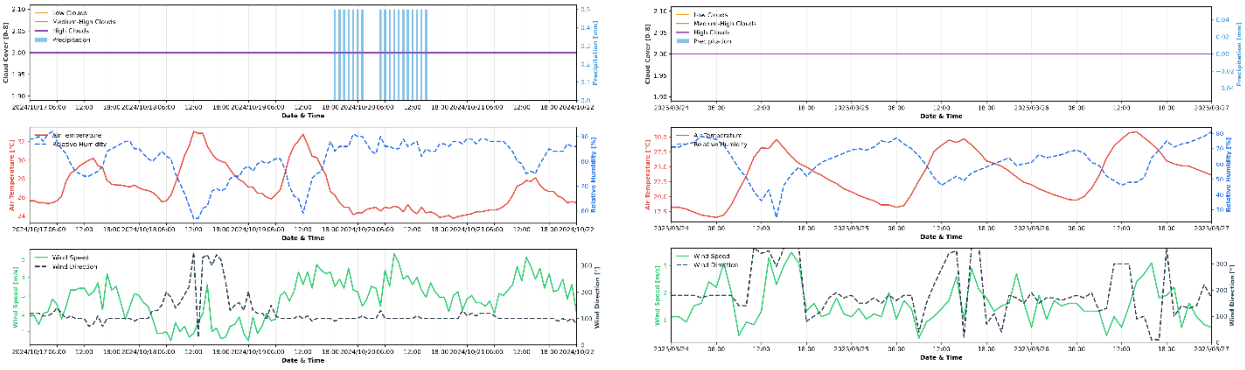

(a) (b)

Figure 3. Meteorological conditions during field measurement V1–V4. (a) October 2024 (V1–V2) and (b) March 2025 (V3–V4). Panels show, cloud cover and precipitation; 6.3m air temperature with relative humidity; 6.3m wind speed with wind direction.

3.3 Validation Analysis

Validation was undertaken by pairing simulated outputs at 1.5m height with co-located field observations and assessing agreement through time-series comparisons, error and association metrics. We evaluated 4 variables (AT, RH, SH, WS); used a complementary set of indices: Coefficient of determination (R^2) to quantify association between simulated and observed values (higher is better). Root-mean-square error (RMSE) for air temperature (AT) to measure error magnitude, Mean absolute percentage error (MAPE) for relative humidity (RH) to express error relative to the observed value. The lower values of RMSE and MAPE are indicated of better simulation performance.

4 Results

4.1 Grid-Size Verification

We evaluated three horizontal resolutions (3, 6, and 9 m) with and without the lake, and analysed five pairwise contrasts, 3 m (lake – no lake), 6 m (lake – no lake), 9 m (lake – no lake), 6 m (lake) – 3 m (lake), and 9 m (lake) – 6 m (lake), across six microclimatic parameters from 6 point's data. Figure 4. shows the spatial distribution of air temperature at 14:00 for the 3, 6, and 9 m grids under lake and no-lake conditions.

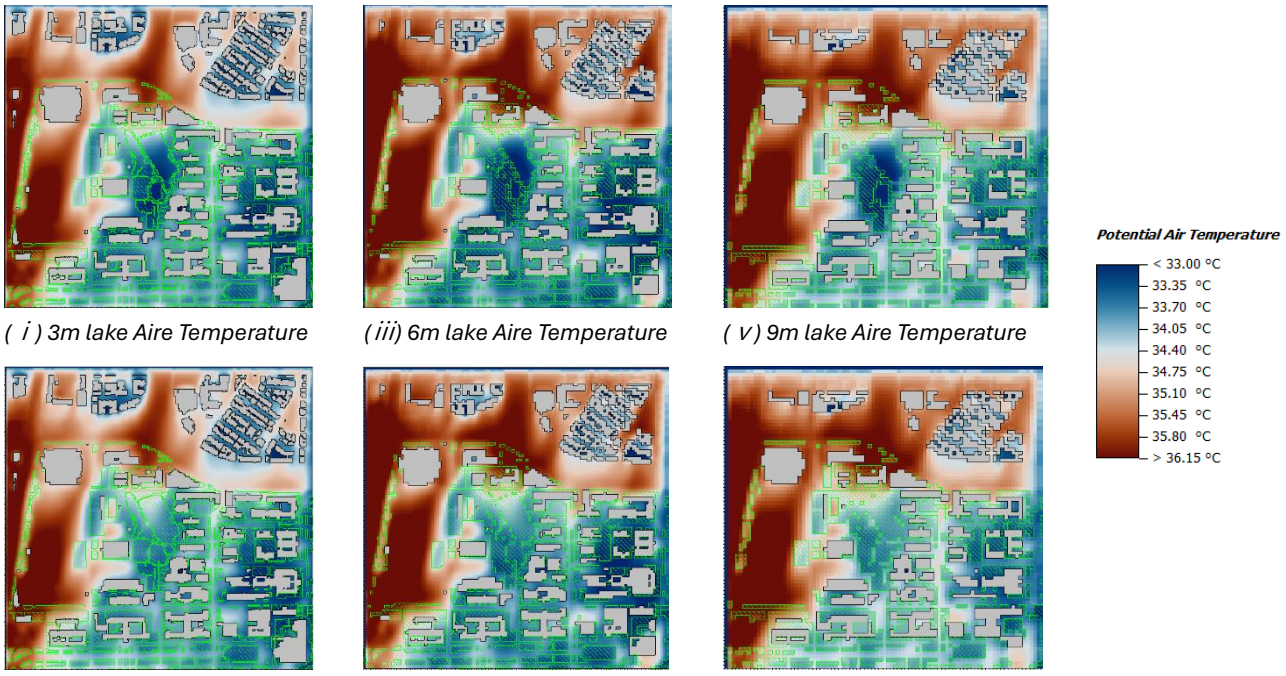

(i) 3m lake Aire Temperature *(iii) 6m lake Aire Temperature* *(v) 9m lake Aire Temperature*

(ii) 3m no-lake Aire Temperature *(iv) 6m no-lake Aire Temperature* *(vi) 9m no-lake Aire Temperature*

Figure 4. 1.5m above ground Air Temperature at 14:00 for six scenarios: (i) 3 m lake, (ii) 3 m no lake, (iii) 6 m lake, (iv) 6 m no lake, (v) 9 m lake, (vi) 9 m no lake.

As Figure 5. show grid-size verification across six microclimatic variables. Each panel shows box-and-whisker summaries for five pairwise comparisons: (a) 3 metre grid with lake minus 3 metre grid without lake, (b) 6 metre with lake minus 6 metre without lake, (c) 9 metre with lake minus 9 metre without lake, (d) 6 metre with lake minus 3 metre with lake, and (e) 9 metre with lake minus 6 metre with lake. Dots indicate values from six reference points; the red line is the median and the blue dot is the mean.

Results from gird size verification

- Air Temperature: lake cooling at all resolutions is similar, mean reductions of 0.14, 0.17, and 0.19 °C for three, six, and nine metres; cross-grid differences are small, with slightly greater variability at finer resolution.
- Mean Radiant Temperature: consistently lower with the lake (means −0.34 to −0.42 °C, medians −0.21 to −0.25 °C); modest cross-grid shift at six minus three metres (mean −0.44 °C) and instability at nine minus six metres, including outliers exceeding +6 °C.
- Relative Humidity: medians near zero in lake versus no-lake comparisons; between lake cases the six-metre grid is +0.64% relative to three metres, while nine metres is −0.78% relative to six metres.
- Specific Humidity: small, consistent decreases (−0.16%, −0.20%, −0.21% for three, six, nine metres); cross-grid contrasts are minimal (about +0.02% for six minus three metres and −0.05% for nine minus six metres).
- Wind Speed: effects are negligible; lake versus no-lake differences are approximately 0.00 m/s; cross-grid offsets are +0.06 and +0.03 m/s for grid six minus three metres and grid nine minus six metres.
- Wind Direction: near-zero means in lake versus no-lake cases (about 0.00° to −0.07°); larger variability in cross-grid comparisons, with a median of +0.28° for six minus three metres and inconsistent behaviour for nine minus six metres (mean +1.36°, median −0.97°, occasional outliers up to ±10°).

For computational cost part, a twenty-four-hour simulation required 84.5 hours at three metres, 13 hours at six metres, and 6.5 hours at nine metres. Overall, the six-metre grid offers the most favourable balance between simulation results and runtime, preserving the lake-cooling signal observed at three metres grid size while reducing computation time by more than sixfold. Resolution influenced variables unevenly. AT and MRT were most responsive and most clearly expressed the lake signal; RH and SH showed modest responses; WS and WD were largely insensitive apart from directional variability in cross-grid comparisons. Balancing accuracy and efficiency, the six-metre grid offers the most favourable trade-off.

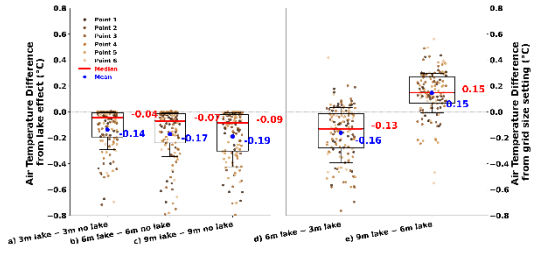

(i) Air Temperature Difference

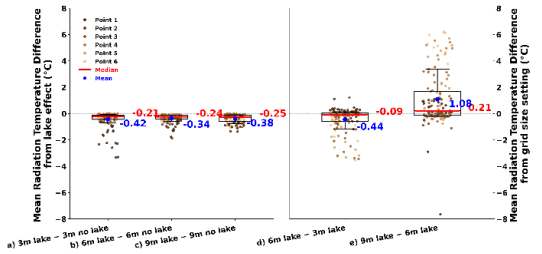

(ii) Mean Radiation Temperature difference

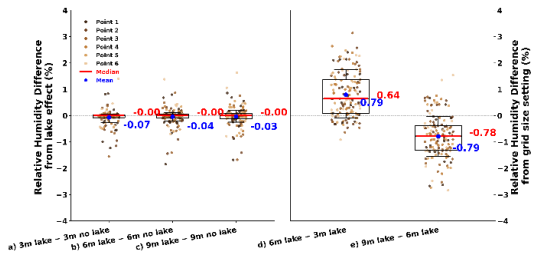

(iii) Relative Humidity Difference

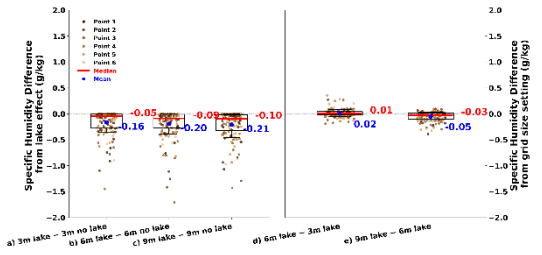

(iv) Specific Humidity Difference

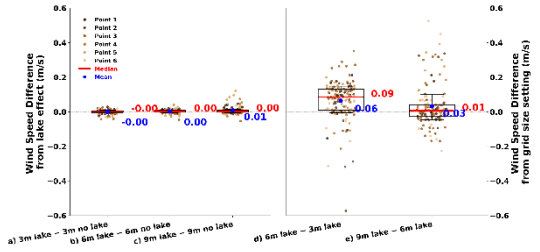

(v) Wind Speed Difference

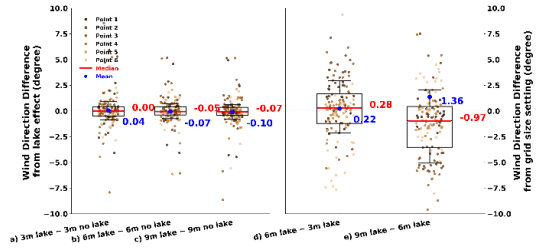

(vi) Wind Direction Difference

Figure 5. Grid-size verification for six microclimatic variables: (i) Air Temperature, (ii) Mean Radiant Temperature, (iii) Relative Humidity, (iv) Specific Humidity, (v) Wind Speed, (vi) Wind Direction. Each panel reports five pairwise contrasts: a) 3 m lake minus 3 m no lake, b) 6 m lake minus 6 m no lake, c) 9 m lake minus 9 m no lake, d) 6 m lake minus 3 m lake, e)9 m lake minus 6 m lake. Dots represent values from six reference points; the red line is the median and the blue dot the mean. Values in a–c indicate effect attributable to the lake, whereas d–e show resolution effects with the lake present.

4.2 Water Body Simulate Validation

4.2.1 Time-Series Comparison

Across the four sites data collect cases, Figure 6. shows the simulations reproduce the diurnal evolution of air temperature with small daytime underestimation, while relative humidity follows observed timing but shows campaign-dependent bias; specific humidity is generally robust in October and weaker in March; and wind speed is consistently overestimated with limited variability. In case V1, sunny, Site A, 39 hr. AT matches the diurnal cycle with slight low bias at daytime peaks. RH tracks observations but is lower at night. SH agrees well. WS is clearly overestimated. Case V2, cloudy, Site B, 39 hr. AT closely follows the damped cycle typical of overcast conditions. RH is broadly consistent but somewhat low in the evening. SH remains stable. WS is again overestimated and shows weak variability. Case V3, sunny, Site B, 22 hr. AT captures heating and cooling with modest underestimation of afternoon maxima. RH timing is good but exhibits a positive nocturnal bias. SH alignment deteriorates. WS overestimation persists, especially when observed speeds are small. Case V4, sunny, Site A, 22 hr. AT follows observations with about a 1 °C low daytime bias. RH is reasonable but positively biased. SH is poorly matched. WS overestimation remains systematic. Overall in four cases, AT performance is strong, RH captures phase with variable bias, SH skill depends on season and site, and WS shows low skill with persistent positive bias.

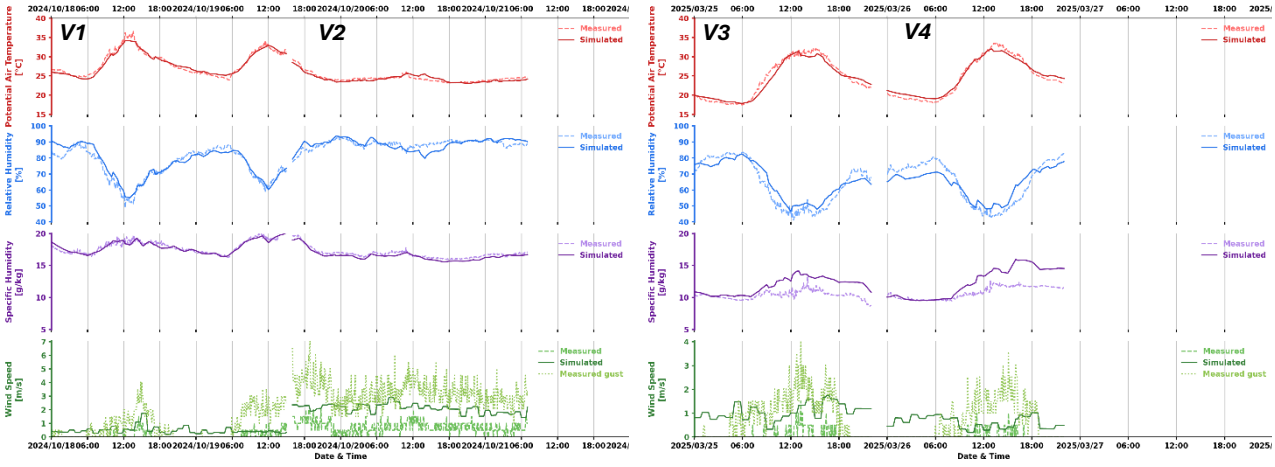

Figure 6. Measured and simulated time series of potential air temperature, relative humidity, specific humidity and wind speed for the validation four cases. The left panel covers 18 to 22 October 2024 (V1 sunny at Site A followed by V2 cloudy at Site B). The right panel covers 25 to 28 March 2025 (V3 sunny at Site B followed by V4 sunny at Site A). Dashed curves are observations and solid curves are ENVI-met simulation results.

4.2.2 Statistical Evaluation

Across the four cases, ENVI-met simulation exhibits strong thermal skill and weak wind skill.

- Air temperature: Agreement is high, with R^2 between 0.77 and 0.99, RMSE below 1.5 °C, and MAE below 1.0 °C. Bias is small, indicating reliable thermal predictions.
- Relative humidity: Performance is case dependent, R^2 ranges from 0.28 to 0.93, typically higher in the sunny case (V1, V3). MAPE is 2–8 %, with a tendency to overestimate at night.
- Specific humidity: Agreement is generally strong in V1, V2 and V4 (R^2 = 0.87–0.94), but weaker in V3 (R^2 = 0.47). RMSE remains <3 g/kg, reflecting robust bulk-moisture representation.
- Wind speed: Correspondence is poor (R^2 = 0.01–0.1), with a systematic positive bias—most evident at the open Site B when observed speeds exceed 2 m/s.

Benchmarking against published thresholds for ENVI-met validation, AT RMSE is within the commonly cited 1.31–1.63 °C range, whereas RH MAPE meets the < 5 % criterion only in the better-performing case. Overall, the metrics corroborate the time-series findings: temperature and moisture are reproduced credibly, while wind variables require caution and, where critical, complementary modelling or measurements. (Shi et al., 2020)

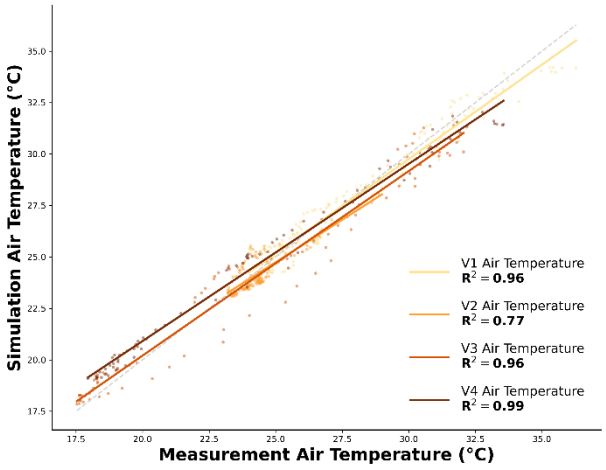

(*i*)

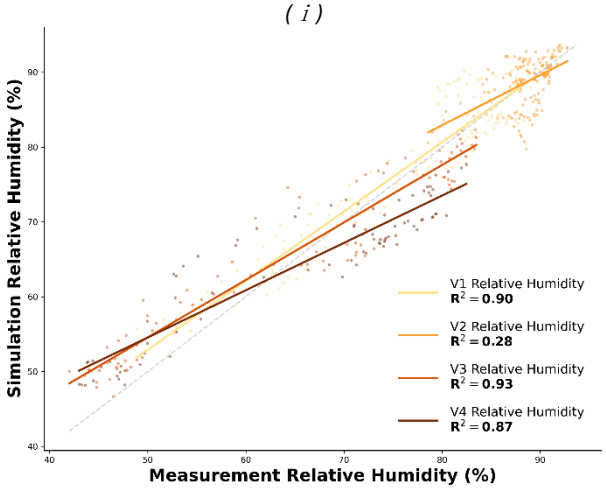

(*ii*)

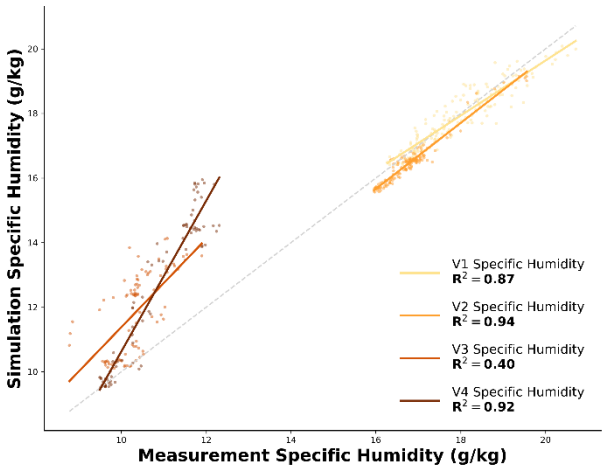

(*iii*)

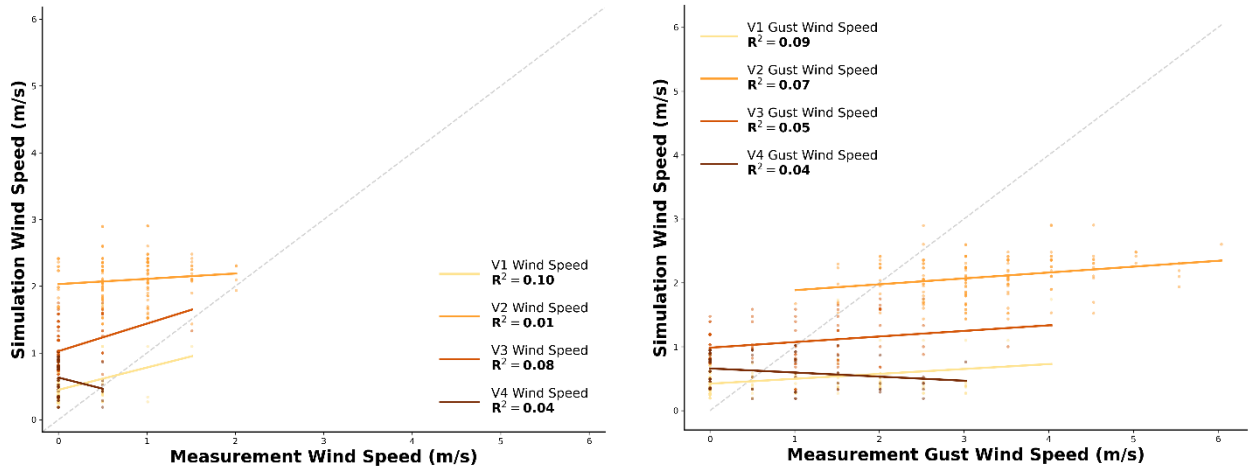

Figure 7. Measurement and simulation compare for the four validated cases. Panels i–v corresponds to (i) Air Temperature, (ii) Relative Humidity, (iii) Specific Humidity, (iv) Wind Speed, and (v) Gust Wind Speed. Points are paired observations and simulations; solid line with the coefficient of determination shown. The grey dashed line indicates the one-to-one reference. Thermal and moisture variables show strong agreement in most case, whereas wind variables display weak correspondence.

Table 4. Validation metrics by case V1–V4 comparing ENVI-met simulations with site collected data; R^2, RMSE, MAE, and MBE for air temperature (°C), relative humidity (%), specific humidity (g/kg), wind speed (m/s), and gust wind speed (m/s). Notes: acceptable benchmarks from prior studies are AT RMSE ≈ 1.31–1.63 °C and RH MAPE < 5%.

variable	*point*	*n*	*R^2*	*RMSE*	*MAE*	*MBE*	*MAPE*	*d*
Air Temperature (°C)	V1	157	0.96	0.67	0.56	-0.12		0.99
	V2	157	0.77	0.54	0.45	-0.16		0.94
	V3	89	0.96	1.04	0.87	-0.22		0.99
	V4	89	0.99	0.90	0.80	0.28		0.99
Relative Humidity (%)	V1	157	0.90		2.58	1.02	3.51	0.97
	V2	157	0.28		2.16	0.07	2.46	0.73
	V3	89	0.93		4.06	1.25	6.92	0.97
	V4	89	0.87		5.23	-1.05	8.28	0.93
Specific Humidity (g/kg)	V1	157	0.87	0.38	0.30	-0.06		0.96
	V2	157	0.94	0.37	0.34	-0.32		0.94
	V3	89	0.40	1.78	1.49	1.48		0.41
	V4	89	0.92	2.17	1.67	1.63		0.65
Wind Speed (m/s)	V1	157	0.10	0.48	0.42	0.37		0.47
	V2	157	0.01	1.42	1.32	1.32		0.34
	V3	89	0.08	1.03	0.97	0.97		0.27
	V4	89	0.04	0.65	0.59	0.57		0.14
Gust Wind Speed (m/s)	V1	157	0.09	1.08	0.82	-0.39		0.47
	V2	157	0.08	1.51	1.27	-1.19		0.45
	V3	89	0.05	0.90	0.76	0.13		0.42
	V4	89	0.04	0.91	0.74	-0.03		0.22

5 Discussion

This study examined ENVI-met's ability to reproduce lake-induced microclimatic cooling on a subtropical campus and quantified the trade-off between grid resolution, predictive accuracy, and computational cost. Across horizontal resolutions from three to nine metres grid, the cooling signal associated with Drunken Moon Lake was consistently apparent in air temperature and mean radiant temperature, whereas relative and specific humidity showed modest shifts and wind variables were comparatively insensitive to resolution. Validation against four monitoring case confirmed high accuracy for air temperature, moderate-to-strong accuracy for humidity, and weak accuracy for wind speed and gust wind speed, characterised by low correlation and systematic positive bias. Importantly, moving from three to six metres preserved the magnitude of the thermal response while reducing runtime by more than six times, indicating a practical resolution–accuracy compromise for campus and district-scale applications.

The diurnal analyses further clarify these patterns (Figure 8.). For most hours of the day the magnitude of lake cooling is similar across the three grid settings, implying that resolution influences variability more than mean effect size. The cooling footprint strengthens during daytime when convective mixing and lake–land temperature contrasts are greater, and it weakens at night when stratification limits advective exchange. This behaviour is visible across variables but is most coherent in air temperature and mean radiant temperature, which are directly affected by radiative forcing and surface heat storage.

These findings are consistent with prior ENVI-met research that reports reliable temperature performance but limited fidelity for wind fields. The present contribution extends the literature by providing validated evidence for blue-infrastructure cooling in a subtropical setting and by offering actionable guidance on grid selection for design practice. For early-stage scenario screening, a six-metre grid enables iterative modelling at feasible runtimes while retaining the salient thermal signal. Given the greater resolution sensitivity of mean radiant temperature, comfort metrics such as PET or UTCI should include explicit checks on grid choice. Where wind-dependent decisions are central—ventilation corridors, wind comfort, or pollutant dispersion—ENVI-met should be complemented by higher-order CFD or targeted on-site measurements.

Limitations for this study includes short monitoring windows at two sites, simplified parameterisations for vegetation and water, and turbulence/drag formulations that likely contribute to wind biases. Future work should extend seasonal coverage, calibrate biophysical parameters, and employ hybrid ENVI-met with other CFD workflows for wind-critical analyses. Overall, ENVI-met provides credible temperature and moisture responses to lake cooling at campus scale, while wind remains a weak point; the six-metre resolution offers a defensible balance between credibility and computational efficiency for climate-sensitive urban design.

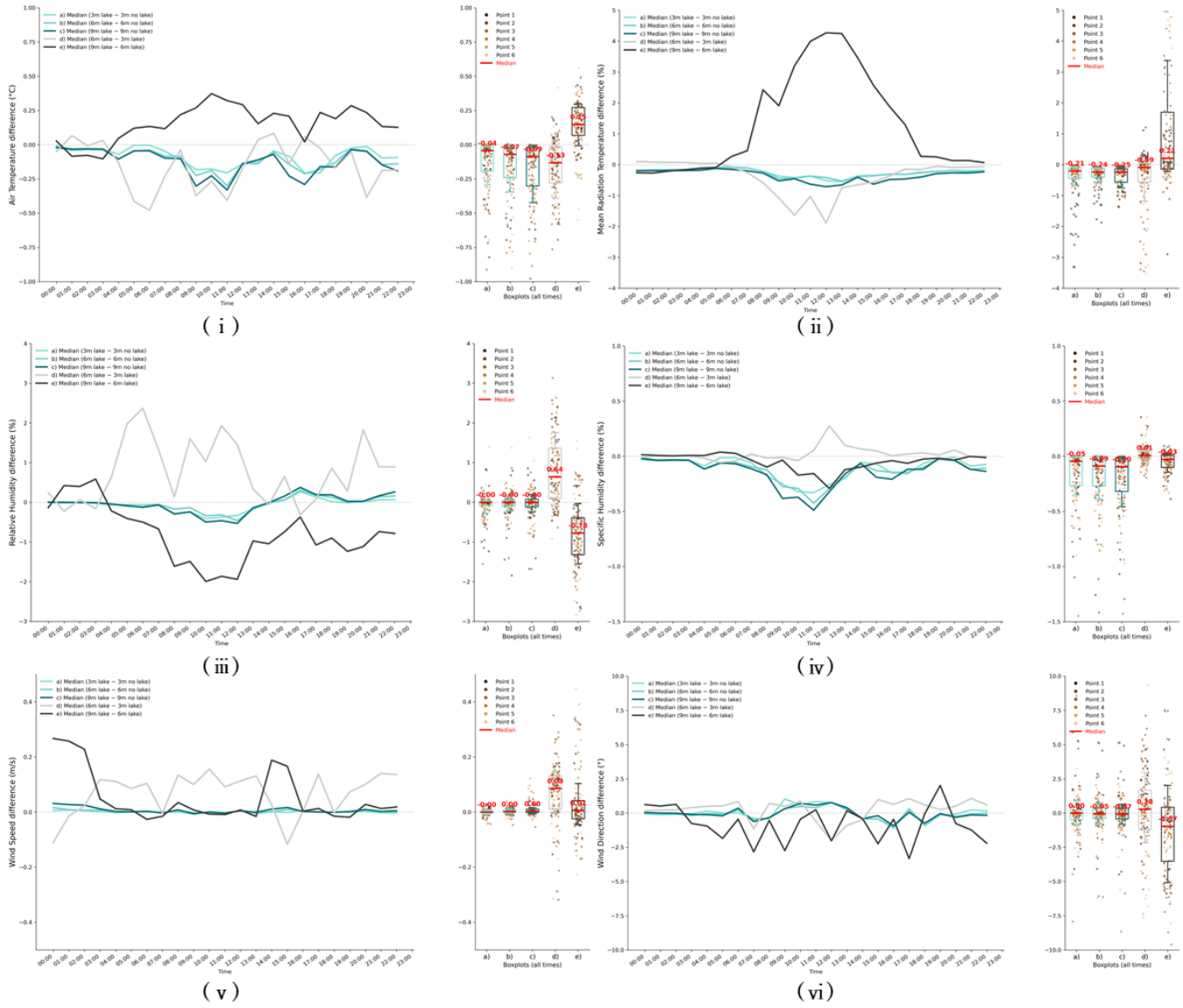

Figure 8. Diurnal signature and distributions of lake-induced differences across three grid resolutions. Panels (i)–(vi) correspond to air temperature, mean radiant temperature, relative humidity, specific humidity, wind speed, and wind direction. For each variable, the left plot shows the hourly median difference for five pairings (3 m lake minus 3 m no-lake; 6 m lake minus 6 m no-lake; 9 m lake minus 9 m no-lake; 6 m lake minus 3 m lake; 9 m lake minus 6 m lake). The right plot presents box-and-whisker summaries of the same differences over all hours and points; dots are individual records, the red line marks the median, and the blue dot marks the mean. Negative values in the lake versus no-lake comparisons indicate cooling.

6 Conclusions

Water cooling effect in AT and MRT is evident at all tested grids; a 6 m resolution preserves this signal while reducing runtime more than sixfold compared to 3 m grid. Across four cases, AT shows high agreement, RH and SH are moderate-to-strong, and wind are weak with positive bias. The study contributes validated blue-infrastructure evidence and operational guidance for resolution choice in subtropical campus settings.

7 Appendix

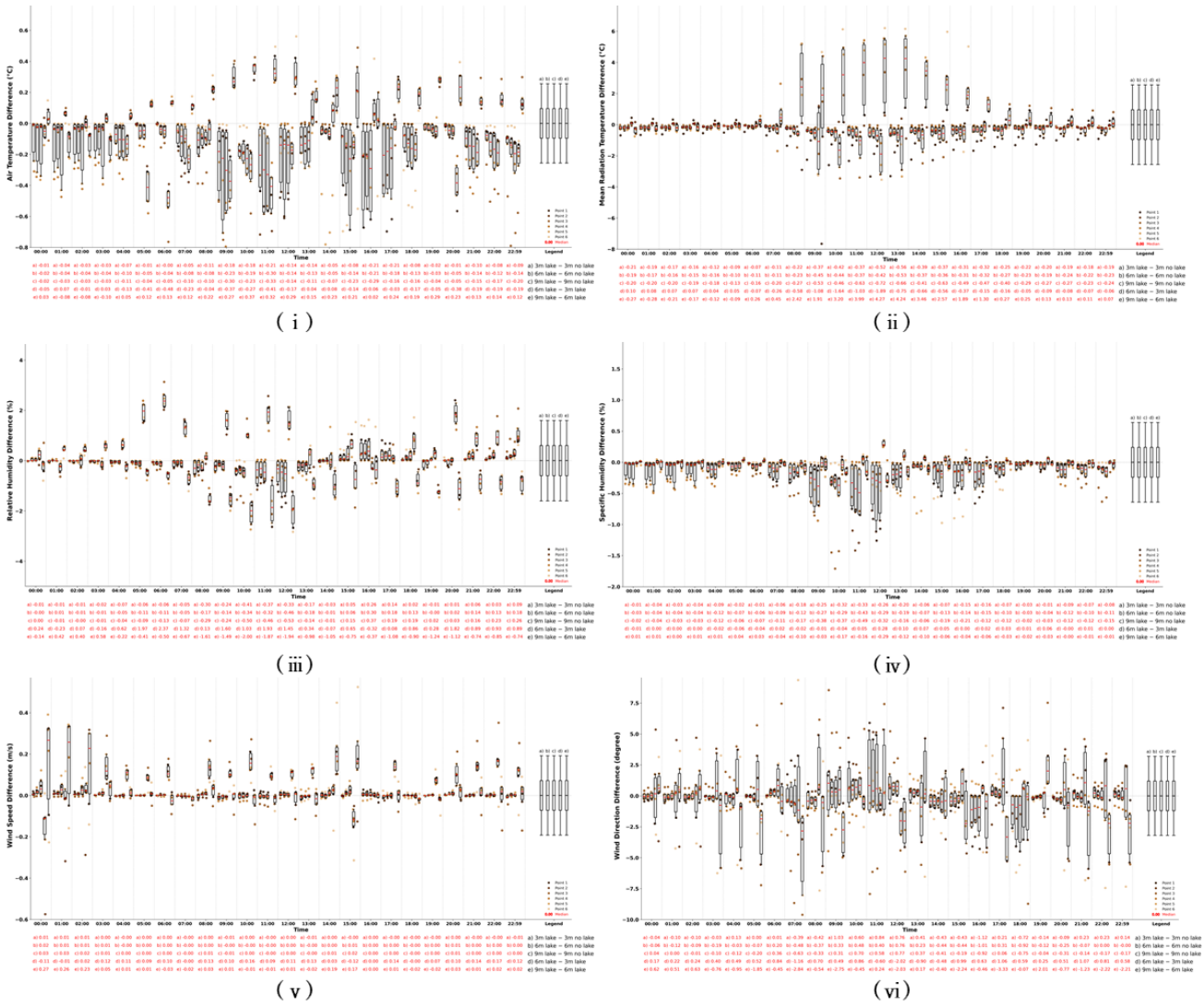

Appendix Figure A1. Hourly distributions of lake-induced differences across three grid resolutions. Panels i–vi correspond to air temperature, mean radiant temperature, relative humidity, specific humidity, wind speed, and wind direction. For each hour, box-and-whisker plots summarise five pairwise contrasts: a) 3 m lake minus 3 m no-lake, b) 6 m lake minus 6 m no-lake, c) 9 m lake minus 9 m no-lake, d) 6 m lake minus 3 m lake, e) 9 m lake minus 6 m lake. Dots are individual records from six reference points; the rightmost bundle in each panel aggregates all hours. Negative values in a–c indicate a cooling effect by the lake; whereas d–e show resolution effects with the lake present.

Acknowledgements

I'm grateful to Professor Ying-Chieh Chan for valuable guidance throughout this study. We also thank National Taiwan University for sharing campus QGIS datasets, and the Department of Atmospheric Sciences, National Taiwan University, for providing access to weather data used in the simulation input. And support from group member on the research road.

Funding

This research received no external funding.

Conflicts of Interest

The authors declare no conflict of interest.

References

Adilkhanova, I., Ngarambe, J., & Yun, G. Y. (2022). Recent advances in black box and white-box models for urban heat island prediction: Implications of fusing the two methods. *Renewable and Sustainable Energy Reviews*, *165*, 112520.

Ampatzidis, P., & Kershaw, T. (2020). A review of the impact of blue space on the urban microclimate. *Science of the total environment*, *730*, 139068.

Le, A.-V., Hip, O.-M., Yang, S.-Y., & Chan, Y.-C. (2024). Sensitivity analysis of building material, ground material, and tree parameters in microclimate simulations. *Urban Climate*, *58*, 102184.

Liao, M.-C., Sung, W.-P., & Chen Shi, Q.-Q. (2024). Comparing Small Water Bodies' Impact on Subtropical Campus Outdoor Temperature: Measured vs. Simulated Data. *Buildings*, *14*(5), 1288.

Liu, F., Liu, J., Zhang, Y., Hong, S., Fu, W., Wang, M., & Dong, J. (2024). Construction of a cold island network for the urban heat island effect mitigation. *Science of the total environment*, *915*, 169950.

Liu, Z., Cheng, W., Jim, C. Y., Morakinyo, T. E., Shi, Y., & Ng, E. (2021). Heat mitigation benefits of urban green and blue infrastructures: A systematic review of modeling techniques, validation and scenario simulation in ENVI-met V4. *Building and Environment*, *200*, 107939.

Pignatta, G., Lim, N., Mughal, M. O., & Acero, J. A. (2018). *Tools for Cooling Singapore: A Guide of 24 Simulation Tools to Assess Urban Heat Island and Outdoor Thermal Comfort*.

Ren, J., Shi, K., Li, Z., Kong, X., & Zhou, H. (2023). A review on the impacts of urban heat islands on outdoor thermal comfort. *Buildings*, *13*(6), 1368.

Richa Jain, T. S. B., Mohammad Arif Kamal. (2022). Environmental Impact and Mitigation Benefits of Urban Heat Island Effect: A Systematic Review. *Architecture Engineering and Science*, *3(4)*, pp.230-237.

Shi, D., Song, J., Huang, J., Zhuang, C., Guo, R., & Gao, Y. (2020). Synergistic cooling effects (SCEs) of urban green-blue spaces on local thermal environment: A case study in Chongqing, China. *Sustainable Cities and Society*, *55*, 102065.

Sinsel, T. (2022). *Advancements and applications of the microclimate model ENVI-met* Dissertation, Mainz, Johannes Gutenberg-Universität Mainz, 2022].

Tian, L., Li, Y., Lu, J., & Wang, J. (2021). Review on urban heat island in China: Methods, its impact on buildings energy demand and mitigation strategies. *Sustainability*, *13*(2), 762.

Tominaga, Y., Sato, Y., & Sadohara, S. (2015). CFD simulations of the effect of evaporative cooling from water bodies in a micro-scale urban environment: Validation and application studies. *Sustainable Cities and Society*, *19*, 259-270.

Toparlar, Y., Blocken, B., Maiheu, B., & van Heijst, G. J. F. (2017). A review on the CFD analysis of urban microclimate. *Renewable and Sustainable Energy Reviews*, *80*, 1613-1640.